Supplementary Figure 1. Histological analysis of WT and *SK3*$^{T/T}$ mouse hearts. A) Hematoxylin and eosin staining of heart sections from three-month-old WT and *SK3*$^{T/T}$ mice. B) Masson's Trichrome staining of heart sections. Neither group demonstrated abnormalities of cardiac structure or abnormal fibrosis.

Supplementary Figure 2. Comparison of *KCNN3* expression in *SK3*$^{T/T}$ mice treated with doxycycline (*SK3*$^{T/T}$ + DOX), and WT mice by RT-PCR. *KCNN3* mRNA levels were quantified in all four cardiac chambers and normalized to β actin expression. Results are expressed as fold change relative to expression levels in WT controls. Error bars represent standard error of mean. *SK3*$^{T/T}$ + DOX mice display suppression of *Kcnn3* expression compared to WT mice in three out of four cardiac chambers. However gene expression was not completely eliminated.

Supplementary Figure 3. Spontaneous atrioventricular dissociation in *SK3*$^{T/T}$ mice. A) Normal sinus rhythm in a WT mouse. B) A representative tracing demonstrating atrioventricular dissociation in an *SK3*$^{T/T}$ mouse. The voltage of the QRS complexes (mV) is depicted on the y axis and time (sec) is depicted on the x axis Abbreviations: mV, millivolts.

Supplementary Figure 4. **Scatter plots of continuous heart rate monitoring in 3-month-old *SK3*$^{T/T}$ and WT mice.** *SK3*$^{T/T}$ mice display a lower average heart rate and increased heart rate variability. Ambulatory monitoring was performed in five *SK3*$^{T/T}$ mice and 2 WT mice. *SK3*$^{T/T}$ mice were designated *SK3*$^{T/T}$ 1-5 and WT mice were designated 1 and 2. The numbers in the parenthesis indicate number of the mouse. The data from *SK3*$^{T/T}$ (1) and WT (1) is included in Figure 4.

Supplementary Figure 5. Immunostaining *SK3*$^{T/T}$ and WT mouse hearts for connexin-43. Paraffin imbedded heart sections from *SK3*$^{T/T}$ and WT mice were stained for connexin-43 and counterstained with Mayer's Hematoxylin Solution. Arrows indicate connexin-43 staining at the intercalated disks of the cells. No quantitative changes in connexin-43 expression were observed between *SK3*$^{T/T}$ and WT hearts.

Supplementary Figure 6. Comparison of body weights in *SK3*$^{T/T}$, *SK3*$^{+/T}$ and WT mice. Box plots demonstrate range of body weight ± standard deviation according to age group. Body weight did not vary significantly in *SK3*$^{T/T}$ mice and *SK3*$^{=/T}$ mice compared to wild type siblings, either at 30 days or 90 days. Abbreviations: 30d, 30-day-old; 90d, 90-day-old.

Supplementary Figure 7. Temperature recordings in *SK3*$^{T/T}$ and WT mice. Temperatures were continuously recorded in five *SK3*$^{T/T}$ and two WT mice throughout the period of ambulatory monitoring. All mice displayed normal temperatures throughout.

Supplementary Figure 8. Immunostaining of atrioventricular nodal sections in *SK3*$^{T/T}$ and WT mouse hearts at 5 months. OCT-embedded heart sections were stained with anti-HCN4 antibody (green). The atrioventricular node is demarcated by the presence of HCN4. Nuclei are stained with DAPI (blue). Scale bar indicates 100 μm. When compared to the WT atrioventricular node, the *SK3*$^{T/T}$ node displays an increased size and disorganized morphology.

Supplementary Figure 9. Potential mechanisms for differential actions of SK3 overexpression in the atrium versus the ventricle. Based on the results of Zhang *et al*, SK3 channel overexpression in

the atrium results in shortening of the atrial action potential which in turn leads to an increased susceptibility to AF. Based on our current results, SK3 channel overexpression in the ventricle results in augmented repolarization heterogeneity. In the atrioventricular node, there is a biphasic effect, initially with shortening of the AVNERP, consistent with the observation of a shortened APD in the atrium, while at later time points, there is prolongation of AVNERP potentially due to repolarization heterogeneity that may in turn underlie the observed heart block. However, we would note that direct recordings from atrioventricular nodal or ventricular myocytes were not performed and thus, this is only a potential model of the effects of SK3 overexpression.

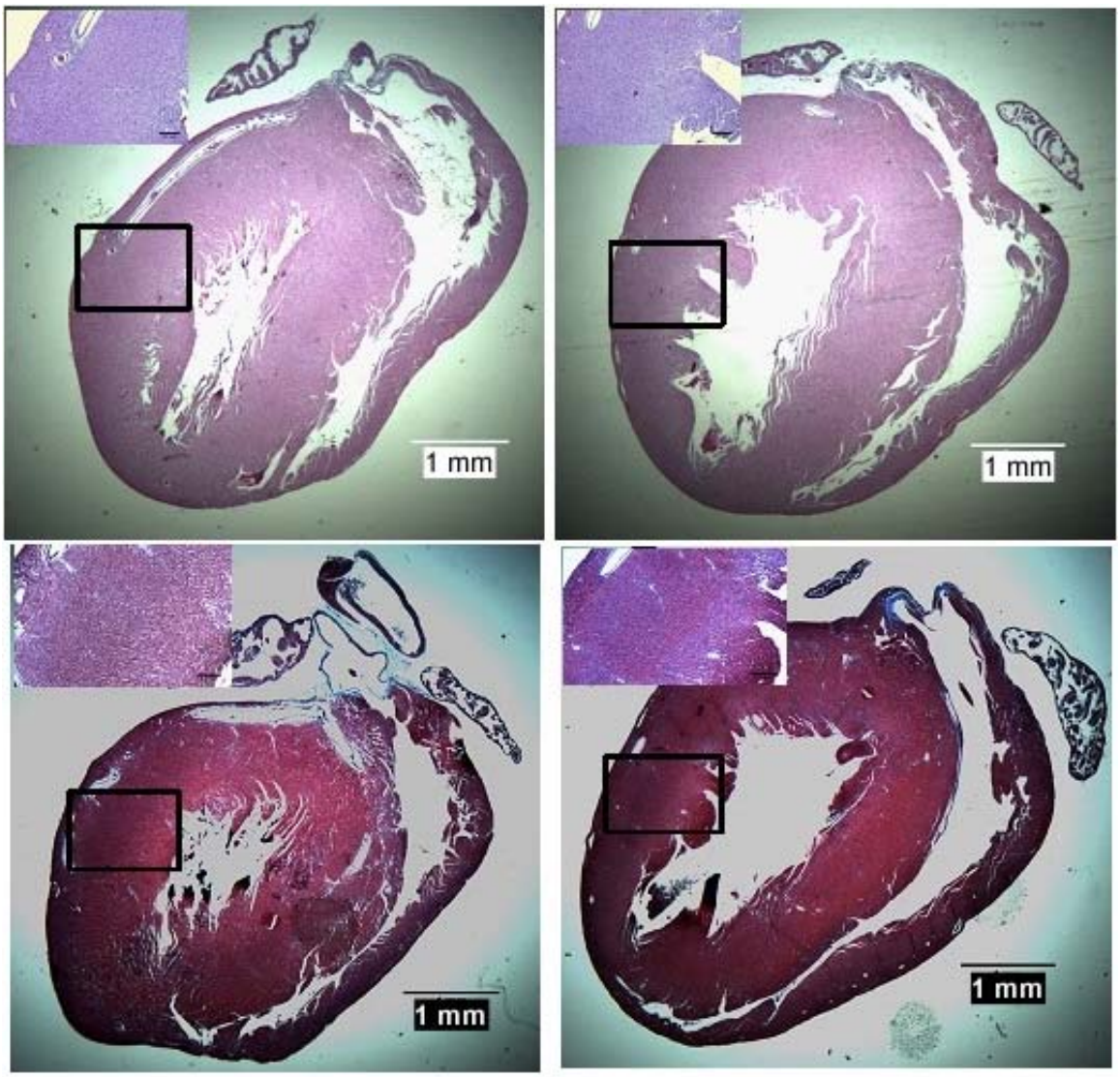
1 mm
1 mm
1 mm
1 mm

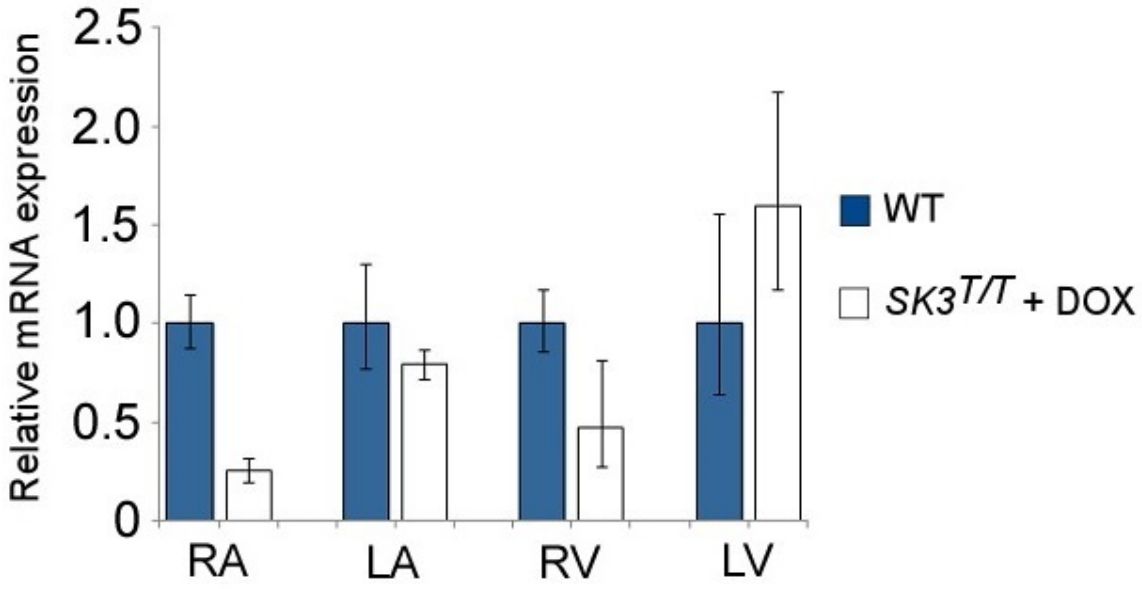
Relative mRNA expression
2.5
2.0
1.5
1.0
0.5
0
RA
LA
RV
LV
WT
SK3T/T + DOX

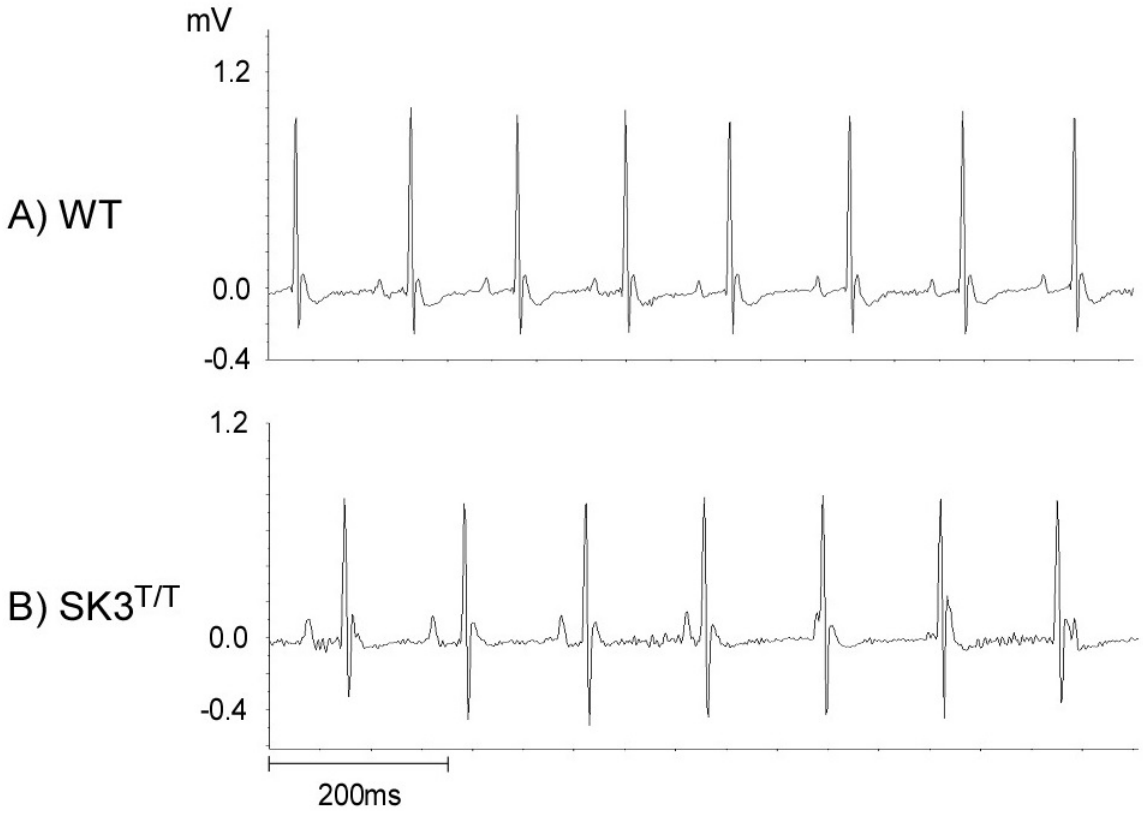
mV
1.2
0.0
-0.4
A) WT
1.2
0.0
-0.4
B) SK3T/T
200ms

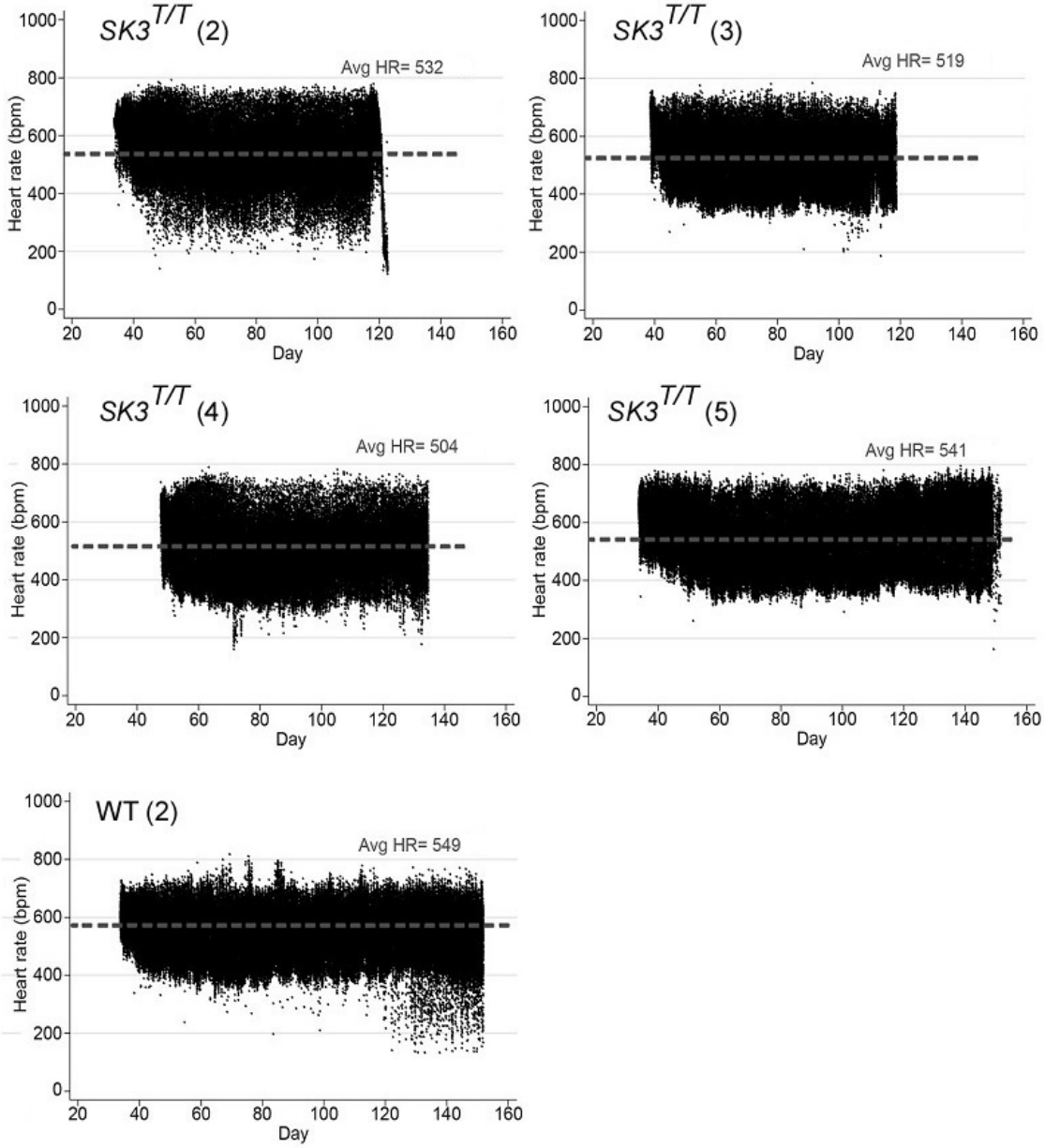
SK3T/T (2)
Avg HR= 532
SK3T/T (3)
Avg HR= 519
SK3T/T (4)
Avg HR= 504
SK3T/T (5)
Avg HR= 541
WT (2)
Avg HR= 549
Heart rate (bpm)
Day
0
200
400
600
800
1000
20
40
60
80
100
120
140
160

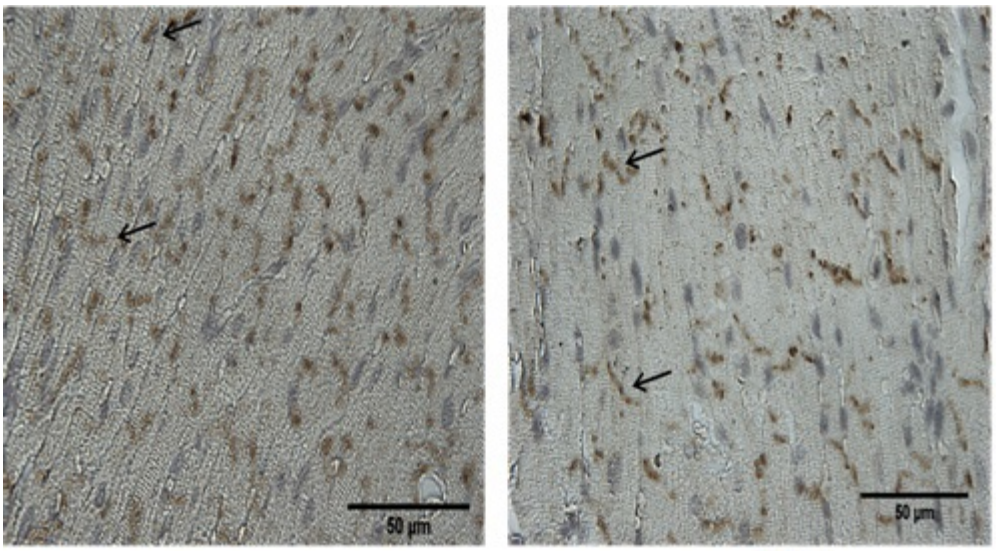

WT $SK3^{T/T}$

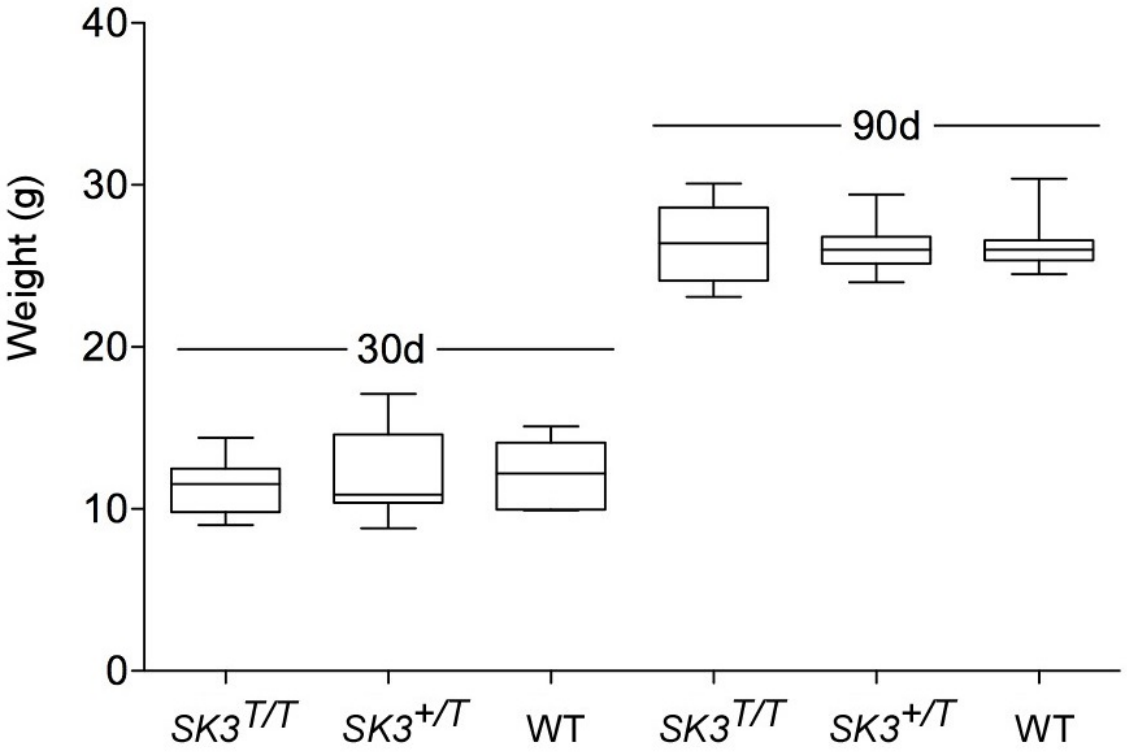
40
30
20
10
0
Weight (g)
30d
90d
SK3T/T
SK3+/T
WT
SK3T/T
SK3+/T
WT

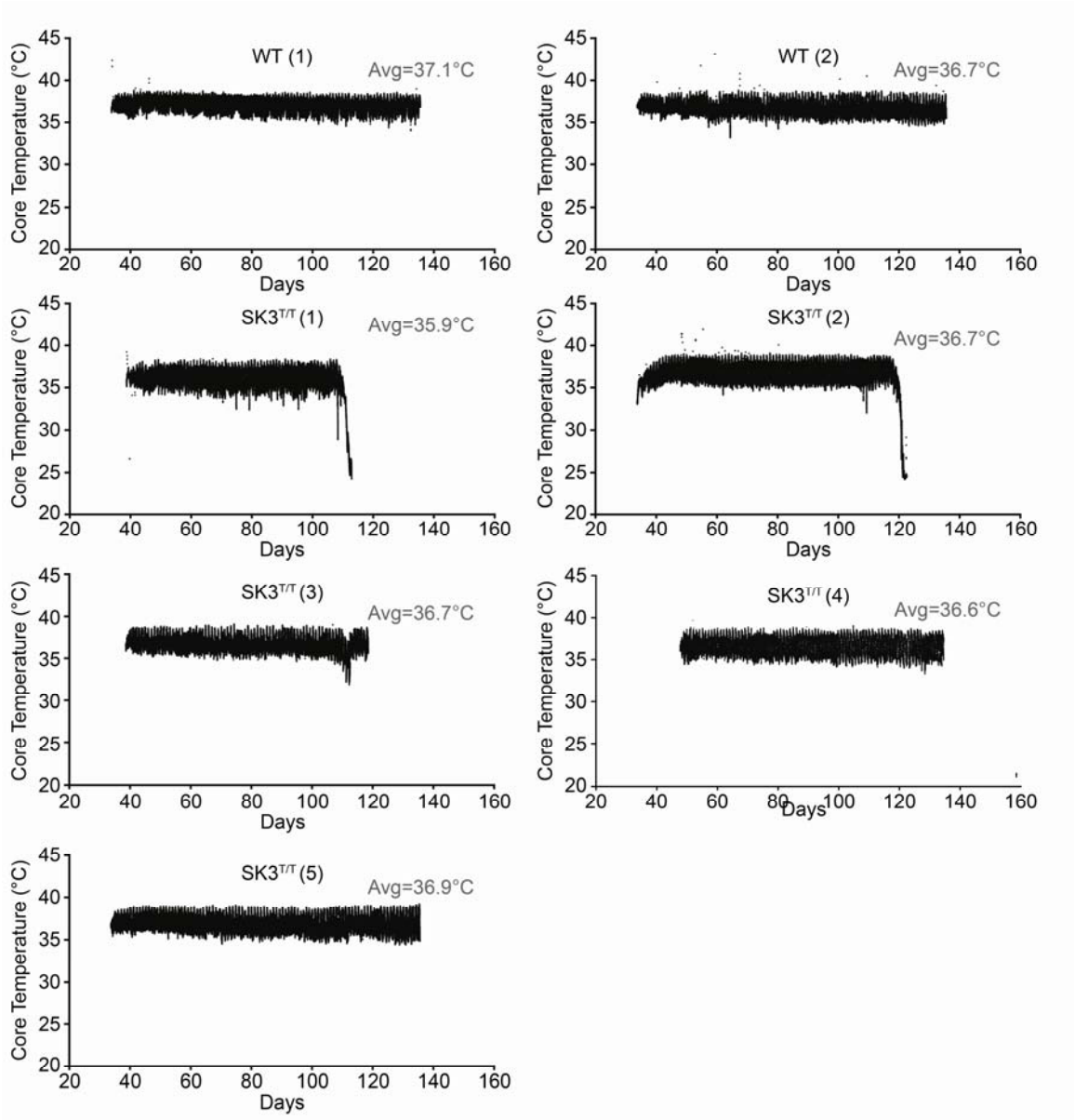
WT (1)
Avg=37.1°C
WT (2)
Avg=36.7°C
SK3T/T (1)
Avg=35.9°C
SK3T/T (2)
Avg=36.7°C
SK3T/T (3)
Avg=36.7°C
SK3T/T (4)
Avg=36.6°C
SK3T/T (5)
Avg=36.9°C
Core Temperature (°C)
Days

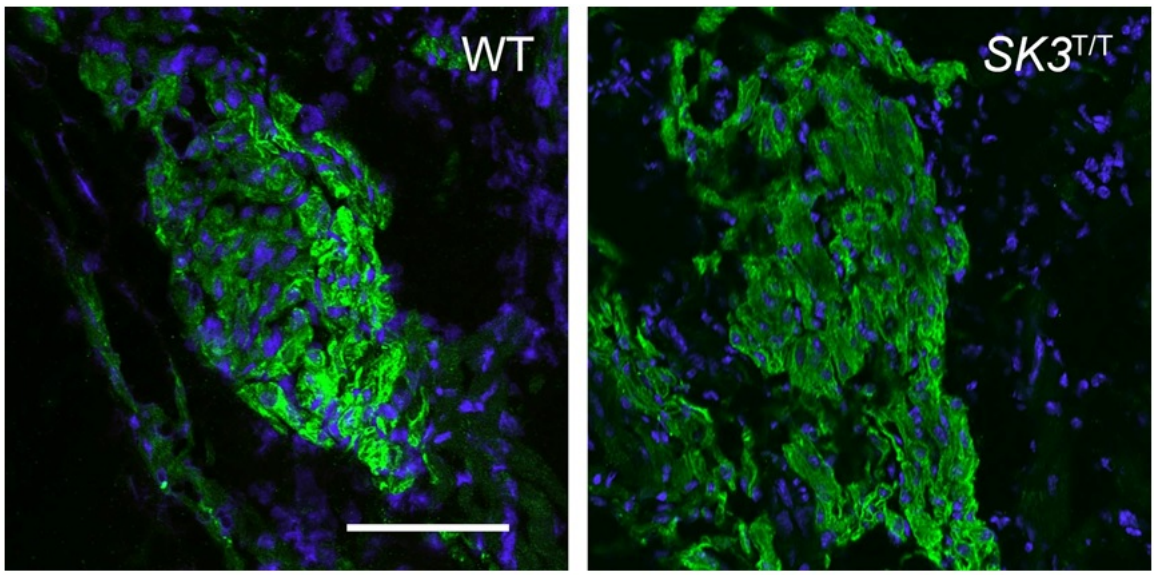
WT
SK3T/T

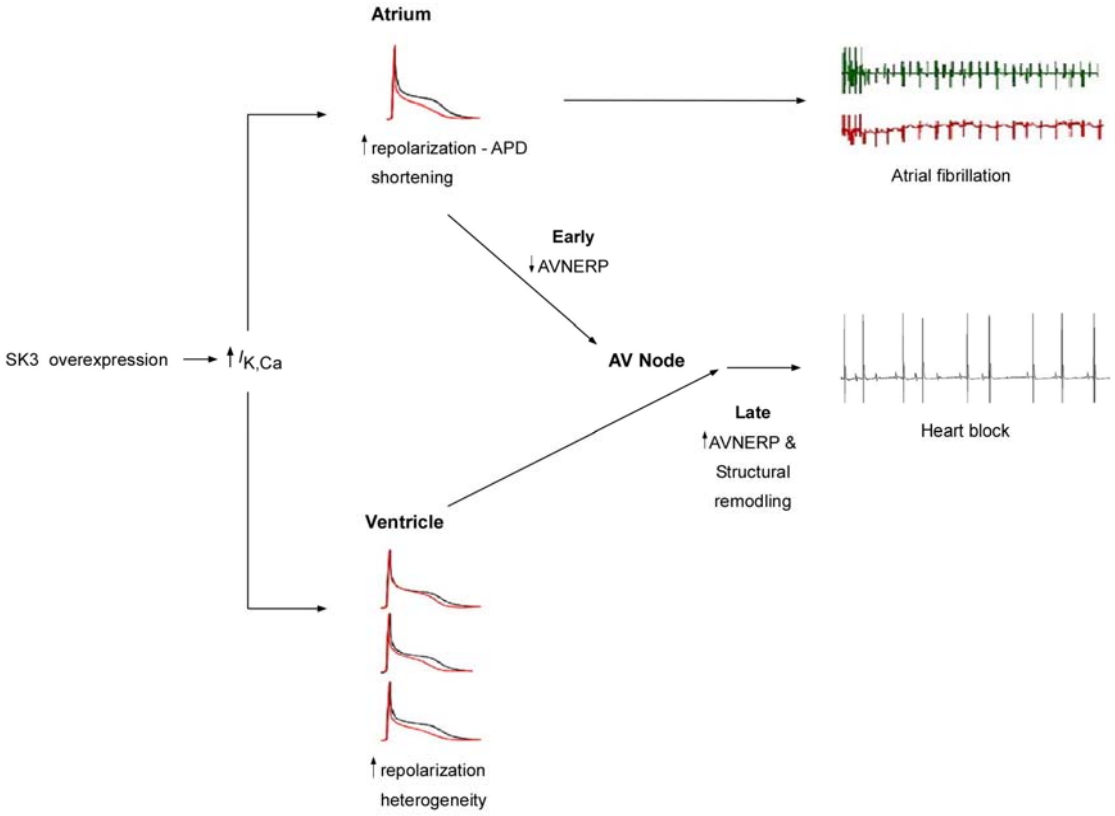
Atrium
repolarization - APD shortening
Atrial fibrillation
Early
AVNERP
SK3 overexpression
$I_{K,Ca}$
AV Node
Late
AVNERP & Structural remodling
Heart block
Ventricle
repolarization heterogeneity